Numerical investigation of melting heat transfer in magnetohydrodynamic flow of hybrid nanofluid (SWCNTs + Ag + Gasoline) over a non-uniform stretching sheet

Narmatha M[1], Rohith Roshan A[2], Sumathi K[3*]

[1]Department of Mathematics, KPR Institute of Engineering and Technology, Coimbatore 641 407, India.
Email: narmathamohan18@gmail.com
[2]Department of Mechanical Engineering, Engineering design division, College of Engineering, Guindy, Chennai 600 025, India. Email: rohithroshanarun@gmail.com
[3]Department of Mathematics, PSGR Krishnammal College for Women, Coimbatore 641 004, India
Email:sumathiarunmath@gmail.com
*Corresponding Author

Received: 19.04.2024 Revised : 20.05.2024 Accepted: 29.05.2024

ABSTRACT
In this work, heat transfer in magnetohydrodynamic hybrid nanofluid flows over a stretching sheet with variable thicknessis examined. Factors such as viscous dissipation, magnetic field, melting and radiation heat are taken into account. Using similarity transformations, governing partial differential equations are transformed into ordinary differential equations. The resulting system of equations are solved by applying shooting method. Velocity and temperature profiles are examined numerically using MATLAB 9.14 as functions of various nondimensional parameters.Variations in skin friction, and Nusselt number are also discussed. The performance of the hybrid nanofluid and nanofluid concerning the base fluid are compared in this study. The effects of relevant parameters, such as volume fraction of nanoparticles, melting heat, velocity ratio, wall thickness, magnetic field, and radiation are numerically analyzed. Magnetic effects reveal significant influences, as the magnetic field increase, results in the minimization of the boundary layer thickness of the sheet. Increase in volume fraction of nano particles, enhances the heat transfer at the boundary.

Keywords: "(SWCNTs + Gasoline oil)"-Nanofluid, "(SWCNTs + Ag + Gasoline oil)"- Hybrid nanofluid, variable thickness sheet, viscous dissipation, MHD, melting heat.

INTRODUCTION

Fluids are frequently utilized in heat transfer devices to carry heat. Due to their lower thermal conductance, convectional fluids including water, motor oil, ethylene oil, kerosine oil, gasoline oil etc., have significantly limited capacity to transfer heat.Thus, scientists and researchers have stated a great deal of importance in developing the fundamental characteristics of thermal liquids. In this way, great interest has been shown by scientists and researchers to study the characteristics of thermal fluids. Thermal conductance of fluids which is mentioned above as suspended nanosized particles (1-100nm) can increase the heat rate in the flow of surface area. Nanoparticles exist from different materials such as oxide ceramics, metals, carbide ceramics, and nitrides (Graphite, carbon nanotubes). In recent days, great interest has been seen in analyzing the heat transport capability through fluids and nanomaterials. These nanoparticle CNT substances have the unique capability of heat conductance more than four times of ordinary substances, they also possess applications innano sensors and atomic transportation. CNTs are fenced from graphene sheets in cylindrical-shaped substances. Based on graphene sheets, CNTs are classified into SWCNTs (cylindrical-shaped carbon substances imprisoned by a single graphene sheet) and MWCNTs (cylindrical-shaped carbon substances imprisoned by more than one graphene sheet) mentioned by Hayat etal.[25]. CNTs are involved in mechanical, tissue engineering, electronics instruments, purification process etc., studied by Volder etal.[5].

Choi etal. [1] initially exhibited in their study about convectional heat transport in the suspension of nanoparticles in fluids with a significantly higher rate of thermal conductance in nanofluids. Properties of a viscous fluid flow and transfer of heat across a nonlinear stretchingsheet are analyzed by Vajravelu [2]. According to Fangetal. [3], the flow on non-flat stretching sheets has many applications in the expulsion processes of metal, plastic, and glass industries. Anjali Devi and Prakash [4] analyzed how radiation heat

affects the heat transfer over variable thickness stretched sheets due to the presence of strong magnetic field.Advancements in CNTs synthesis, purification and modification have enabled their use in thin -film coatings. Even though they may not meet all requirements for certain applications such as yarns, sheets of CNTs have shown their potential in supercapacitors, actuators and electromagnetic protectionas mentionedby Volder etal. [5]. Muhammad etal. [6] explored numerically about characteristics of convectional heat transport and viscous dissipation in the hybrid nanofluid flow. Turkyilmazoglu [7] investigated heat generation effects, absorption and radiation among the natural convective flow with the various nanomaterials like titanium oxide, alumina, copper, copper oxide and silver with water as basefluid.The characteristics of the flow through the incompressible boundary layer of nanofluid-saturated porous media across a semi-infinite stretched surface under the influence of magnetic effect and chemical reaction is studied by MamiNassima and Mohamed Najib Bouaziz [8]. Sekh etal. [9] studied the combined effect of nanoparticles and the uniform magnetic field on the flow of slip blood flowing in arterial vessels. Goud
etal. [10] dealt with the boundary layer flow of a magnetohydrodynamic fluid over a stretching sheet and consideredthe effects of heat radiation. Poply Vikas [11] provided valuable insights to manage the heat transportation rate and fluid velocity relevant to many applications inindustrial and manufacturing processes. Prasad etal. [12] examinedthe effects of Brownian motion, thermophoresis, suction and injection in MHD nanofluid over an elongate sheet with variable thickness. The computation of experimental work was carried outexperimentally studied bySuresh etal. [13]. Ahmad etal. [14] specifically examined the movement of a thin needle with varying thickness with a surface heat flux in the double phase of hybrid nanofluids theoretically. Devi and Devi [15] discussed the advanced version of hybrid nanofluidsin convectional heat transfer fluids and studied how it is effectively utilized to maximize the rate of heat transmission.Hayat and Nadeem [16]presented a clear prediction of the influence of thermal conductivity.Wainietal. [17] analyzed heat transportation of Ag-CuO/water.

Melting heat has excited the experts' interest in manufacturing environments.Because of its various applications in industrial processes like semiconductor preparation, frozen ground thawing, magma solidification etc.,the significanceof melting phenomena in the flow of extended surfaces are explored byRobert [18]. Hayat etal. [19] discussed about melting heat transport of carbon nanotubes flowing at stagnationpoint over a variable thickened surface. Fazle Mabood etal. [20] studied viscous dispersion of heat transfer from a base fluid to a stretched sheet during MHD boundary layer melting heat. Zainal etal. [21] considered thermal radiation with flow of MHD along heat transport of hybrid nanofluid over a flat moving surface.Anum Shafiq etal. [22] explained how carbon nanotubes are induced on MHD stagnation point over variable thicken surfaces. Aisyah Jaafar etal. [23] investigated the behavior of a hybrid nanofluid subject to nonlinear extending/contracting sheet and analyzed the effects of magnetohydrodynamics, thermal radiation and suction. Ramamoorthi et al. [24] studied flows of different types of hybrid nanofluids over a moving vertical plate in a magnetic field and porous medium. Utilization of hybrid nanofluids of silver, titanium oxide and water flow over an exponentially stretching surface inresultof various effects isreviewed by Abdul Basit etal. [26]. Jamrusetal. [27] focused to study the fluid flow and heat transfer in the stagnation region of a thermally stratified ternary hybrid nanofluid over a permeable stretchable/shrinkable sheet and the effects of magnetohydrodynamicsandslip boundary conditions are analyzed numerically. Muhammad etal. [25] proceeded with the stagnation point of a hybrid nanofluid flow over a variable-thickness stretching sheet considering viscous dissipation and melting heat transfer.

The main objective of this work is to examine magnetohydrodynamic (MHD) effects of hybrid nanofluid over a stretching sheet with variable thickness. The rate of heat transport is mentioned in the form of viscous dissipation and melting heat radiation and magnetic field is worked. Hybrid nanofluid involves the suspension offirst nanomaterialas SWCNTs and second nanomaterial as Ag (Silver) in basefluidgasoline. The governing equations for flow and heat transferare framed as PDEs and are converted as first order ODEs,then solved using BVP4C (shooting method). Various physical parameters based on temperature and velocity are discussed in graphs.

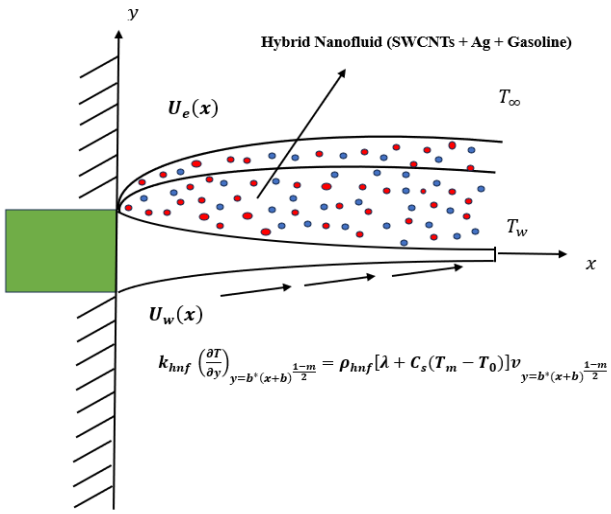

Figure 1. Physical Description of flow field

Flow description

Consider a flow of magneto hydrodynamic fluid over a variable-thickness stretched sheet. The aforementioned y-axis is perpendicular to the stretching sheet in cartesian coordinates and the sheet is stretched along the direction of the x-axis with the stretching velocity $U_W = U_0(x+b)^m$. Thickness of sheet is taken as $y = b^*(x+b)^{\frac{1-m}{2}}$, indicating the sheet thickness along the x-axis.

Table 1. Thermal characteristics of nanoparticles [25]

Nanoparticle/Thermo physical properties	$\rho\left(\frac{kg}{m^3}\right)$	$k\left(\frac{W}{mK}\right)$	$C_p\left(\frac{J}{kgK}\right)$	Pr
SWCNTs	1600	3000	796	-
Ag	10490	235	429	-
Gasoline oil	750	0.114	425	9.4

The governing equations are

$$\frac{\partial u}{\partial x} + \frac{\partial v}{\partial y} = 0 \quad (1)$$

$$u\frac{\partial u}{\partial x} + v\frac{\partial u}{\partial y} = U_e\frac{dU_e}{dx} + \upsilon_{hnf}\frac{\partial^2 u}{\partial y^2} - \frac{\sigma B_0^2}{\rho_{hnf}}(U - U_e) \quad (2)$$

$$u\frac{\partial T}{\partial x} + v\frac{\partial T}{\partial y} = \alpha_{hnf}\frac{\partial^2 T}{\partial y^2} + \frac{\upsilon_{hnf}}{(\rho C_p)_{hnf}}\left(\frac{\partial u}{\partial y}\right)^2 - \frac{\partial q_r}{\partial y} \quad (3)$$

and the corresponding boundary conditions are,

$$u = U_w(x) = U_0(x+b)^m, v = 0, T = T_m \text{ aty} = b^*(x+b)^{\frac{1-m}{2}}$$
$$u \to U_e(x) = U_\infty(x+b)^m, T \to T_\infty \text{ at } y \to \infty \quad (4)$$

Melting heat conditions are considered as [16];

$$k_{hnf}\left(\frac{\partial T}{\partial y}\right) = \rho_{hnf}[\lambda + C_s(T_m - T_0)]v_{y=b^*(x+b)^{\frac{1-m}{2}}} \quad (5)$$

By considering theRosseland Approximation,

$$q_r = -\frac{4\sigma^*\partial T^4}{3k^*\partial y} = -\frac{16\sigma^*}{3k^*}T^3\frac{\partial T}{\partial y} \quad (6)$$

k^* is mentioned as coefficient of absorption, σ^* is mentioned as Stefan-Boltzmann constant and T^4 is used to express taylor series upto T_∞ is

$$T^4 = 4T_\infty^3 T - 3T_\infty^4 \quad (7)$$

We choose the transformations,

$$\eta = \sqrt{\frac{m+1}{2\upsilon_f}U_0(x+b)^{m-1}}.y, \qquad \psi = \sqrt{\frac{2\upsilon_f}{m+1}U_0(x+b)^{m+1}}f^*(\eta),$$

$$\theta^*(\eta) = \frac{T-T_m}{T_\infty - T_m} \qquad u = U_0(x+b)^m f^{*'}(\eta),$$

$$v = -\sqrt{\frac{(m+1)\upsilon_f}{2}U_0(x+b)^{m-1}}\left(f^*(\eta) + \eta f^{*'}(\eta)\frac{m-1}{m+1}\right) \tag{8}$$

By substituting the above similarity transformations in equations(1)-(3), we get,

$$\frac{A_{11}}{(1-\varphi_1)^{2.5}(1-\varphi_2)^{2.5}}f^{*'''} + f^*f^{*''} + \frac{2m}{m+1}A^2 - \frac{2m}{m+1}f^{*'^2} - M^2\left(f^{*'} - A\right) = 0 \tag{9}$$

$$\left(\frac{k_{hnf}}{k_f} + \frac{4}{3}Rd\right)\theta^{*''} + \frac{Pr\,Ec}{(1-\varphi_1)^{2.5}(1-\varphi_2)^{2.5}}f^{*''^2} - B_{11}Pr\theta^{*'}f^* = 0 \tag{10}$$

The associated boundary conditions are

$$f^{*'}(\alpha) = 1, \theta^*(\alpha) = 0, \frac{k_{hnf}}{k_f}\beta\theta^{*'}(\alpha) + A_{11}\left(Prf^*(\alpha) + \alpha\frac{m-1}{m+1}\right) = 0 \text{ at } \alpha = b^*\sqrt{\frac{m+1}{2\upsilon_f}U_0}$$

$$f^{*'}(\infty) \to A, \theta^*(\infty) \to 1 \text{ as } \alpha \to \infty \tag{11}$$

where

$$A_{11} = \frac{1}{(1-\varphi_2)\left((1-\varphi_1)+\varphi_1\frac{\rho_{s1}}{\rho_f}\right)+\varphi_2\frac{\rho_{s2}}{\rho_f}} \tag{12}$$

$$B_{11} = \left(\left(1-\varphi_2\right)\left(\left(1-\varphi_1\right)C_{pf} + \varphi_1\frac{(\rho C_p)_{s2}}{\rho_f}\right)\right) + \varphi_2\frac{(\rho C_p)_{s1}}{\rho_f} \tag{13}$$

Prime represents a derivative forη and wall thickness is $\alpha = \eta = b^*\sqrt{\frac{m+1}{2\upsilon_f}U_0}$ which gives a flat surface. Here we define $f^*(\eta) = f(\eta - \alpha) = f(\xi)$. Hence equations (9) and (10) become

$$\frac{A_{11}}{(1-\varphi_1)^{2.5}(1-\varphi_2)^{2.5}}f''' + ff'' + \frac{2m}{m+1}(A^2 - f'^2) - \frac{2M^2}{m+1}(f' - A) = 0 \tag{14}$$

$$\left(\frac{k_{hnf}}{k_f} + \frac{4}{3}Rd\right)\theta'' + \frac{Pr\,Ec}{(1-\varphi_1)^{2.5}(1-\varphi_2)^{2.5}}f''^2 - B_{11}Pr\theta'f = 0 \tag{15}$$

with boundary conditions

$$f'(0) = 1, \theta(0) = 0, \frac{k_{hnf}}{k_f}\beta\theta'(0) + A_{11}\left(Prf(0) + \alpha\frac{m-1}{m+1}\right) = 0,$$

$$f'(\infty) \to A, \theta(\infty) \to 1 \text{ when } \xi \to \infty \tag{16}$$

The nondimensional parameters involved are

$$A = \frac{U_\infty}{U_0}, \alpha = b^*\sqrt{\frac{m+1}{2\upsilon_f}U_0}, Pr = \frac{\mu C_p}{k}, Ec = \frac{U_0^2(x+b)^{2m}}{(T_\infty - T_m)C_{p_f}}, \beta = \frac{C_{p_f}(T_\infty - T_m)}{\lambda + C_s(T_m - T_0)},$$

$$M^2 = \frac{\sigma B_0^2(x+b)^{m-1}}{\rho_f U_0}, Rd = \frac{4\sigma T^3}{kk_f} \tag{17}$$

Expression for skin friction

The skin friction coefficient(C_f)is defined as

$$C_f = \frac{\tau_w}{\rho_f U_w^2} \tag{18}$$

$$\tau_w = \mu_{hnf}\left(\frac{\partial u}{\partial y}\right)_{y=b^*\sqrt{\frac{m+1}{2\upsilon_f}U_0}} \tag{19}$$

Expression for local Nusselt number

Local Nusselt number(Nu_x)is defined as

$$Nu_x = \frac{(x+b)q_w}{k(T_\infty - T_m)} \tag{20}$$

$$q_w = -k_{hnf}\left(\frac{\partial T}{\partial y}\right)_{y=b^*\sqrt{\frac{m+1}{2\upsilon_f}U_0}} \tag{21}$$

Substitute equations (8),(19) and (21) in equations (18) and (20) we get,

$$C_f\sqrt{Re_x} = \frac{1}{(1-\varphi_1)^{2.5}(1-\varphi_2)^{2.5}}\sqrt{\frac{m+1}{2}}f''(0) \tag{22}$$

$$\frac{Nu_x}{\sqrt{Re_x}} = -\frac{k_{hnf}}{k_f}\sqrt{\frac{m+1}{2}}\theta'(0) \tag{23}$$

then local Reynolds number defined as $\mathrm{Re}_x = \frac{U_0(x+b)^{m+1}}{\upsilon_f}$.

Models of nanofluid

For nanofluid we obtained [16];

$$\mu_{nf} = \frac{\mu_f}{(1-\varphi_1)^{2.5}}$$

$$\upsilon_{nf} = \frac{\mu_{nf}}{\rho_{nf}}$$

$$(\rho C_p)_{nf} = (1-\varphi_1)(\rho C_p)_f + \varphi_1(\rho C_p)_{s1}$$

$$\rho_{nf} = (1-\varphi_1)\rho_f + \varphi_1\rho_{s1}$$

$$\frac{k_{nf}}{k_f} = \frac{k_{s1} + (n-1)k_f - (n-1)\varphi_1(k_f - k_{s1})}{k_{s1} + (n-1)k_f + \varphi_1(k_f - k_{s1})}$$

Models of hybrid nanofluid

For hybrid nanofluid we have [16];

$$\mu_{hnf} = \frac{\mu_f}{(1-\varphi_1)^{2.5}(1-\varphi_2)^{2.5}}$$

$$(\rho C_p)_{hnf} = (1-\varphi_2)\left((1-\varphi_1)(\rho C_p)_f + \varphi_1(\rho C_p)_{s1}\right) + \varphi_2(\rho C_p)_{s2}$$

$$\rho_{hnf} = (1-\varphi_2)\left((1-\varphi_1)\rho_f + \varphi_1\rho_{s1}\right) + \varphi_2\rho_{s2}$$

$$\frac{k_{hnf}}{k_f} = \frac{k_{s2} + (n-1)k_f - (n-1)\varphi_2(k_f - k_{s2})}{k_{s2} + (n-1)k_f + \varphi_2(k_f - k_{s2})}$$

$$\frac{k_{bf}}{k_f} = \frac{k_{s1} + (n-1)k_f - (n-1)\varphi_1(k_f - k_{s1})}{k_{s1} + (n-1)k_f + \varphi_1(k_f - k_{s1})}$$

Cylindrical-shaped nanoparticles are considered for analysis, n is taken as 6 for both hybrid nanomaterials and nanofluids.

METHODOLOGY

The shooting technique (BVP4C) is developed to find solutions for governing flow expressions (ODEs).As a result, we follow the steps listed below.

$$h_1 = f$$

$$h_2 = f_1' = f'$$

$$h_3 = f_2' = f''$$

$$h_4 = f_3' = f'''$$

$$= -\frac{(1-\varphi_1)^{2.5}(1-\varphi_2)^{2.5}}{A_{11}}\left(f_1 f_3 - \frac{2m}{m+1}(f_2)^2 + \frac{2m}{m+1}A^2 + \frac{2}{m+1}M^2(f_2 - A)\right)$$

$$h_6 = f_5' = \theta'' = \frac{1}{\left(\frac{k_{hnf}}{k_f} - \frac{4}{3}Rd\upsilon_f\right)}\left(B_{11}\mathrm{Pr}f_1 f_6 + \frac{\mathrm{Pr}\,Ec}{(1-\varphi_1)^{2.5}(1-\varphi_2)^{2.5}}(f_3)^2\right)$$

$$h_2(0) = 1, h_5(0) = 0,$$

$$\frac{k_{hnf}}{k_f}\beta h_6(0) + A_{11}\left(\mathrm{Pr}h_1(0) + \alpha\left(\frac{m-1}{m+1}\right)\right) = 0,$$

$h_2(\infty) \to A, h_5(\infty) \to 1$ as $\xi \to \infty$.

Numerical Analysis

This study investigates the impacts on temperature, local Nusselt number, skin friction coefficient, and velocity using graphical depiction. Throughout this study $\varphi_1 = \varphi_2 = 0.0$ for base fluid, $\varphi_2 = 0.0$ for nanofluid φ_1 and φ_2 are adjusted for hybrid nanofluid.

Influence of significantparameters $(\boldsymbol{\varphi_1, \varphi_2, \beta, A, \alpha, m, M})$on velocity profile on $\mathbf{f'(\eta)}$.

Figure2.llustrates the validation ofvolume fraction of nanomaterial SWCNTs, in view ofthe previouswork by Muhammad etal. [25]. Figure3 and 4represent the effects of$\varphi_1 \in [0.1, 0.4]$ and $\varphi_2 \in [0.1, 0.4]$ on $f'(\eta)$. Here $f'(\eta)$increases with increasingφ_1 and φ_2. In comparison to nanofluid, hybrid nanofluid is more effective due to the involvement of a fractional volume of suspended particles.Figure5. Shows the

variations of $f'(\eta)$ due to the enhancement of$\beta \in [0.1, 0.4]$. It is found that $f'(\eta)$varies directly with β. Increased values result in the movement of fluid particles, causing the surface to melt and move towards the hotter fluid above it. Adding more amount of fluid particles enhances the velocity of the fluid. The impacts of β for hybrid nanofluid are more compared to the nanofluid.

Figure 6. Illustrates the impact of$A \in [0.8, 1.2]$ on the velocity profile, showing that $f'(\eta)$ exhibits enhancement with increasing A values. Moreover, when $A = 1$, the boundary layer will not be present.At the same time $A > 1$ and $A < 1$ respectively indicates boundary thickening and thinning based on the velocity ratio.Figure7demonstrates variation in the velocity profile within the range of $\alpha \in [0.2, 0.8]$. The influence of wall thickness(α) seems more pronounced in hybrid nanofluids compared to standalone nanofluids.Figure8. mentions the influence of $m < 1$ on velocity profile, indicating that it decreases as m decreases further, corresponding to lower fluid velocity. The study also illustrates fluctuations in the velocity profile for $m \in [0.2,0.8]$. Importantly, the effect of wall thickness is more noticeable in hybrid nanofluids when compared to nanofluids without the hybrid component.Figure9 Shows the significance of the magnetic field strength within the range$M \in [0.1,0.4]$. Typically, higher estimators lead to a decrease in the surrounding layer, which is closely associated with changes in the velocity profile.

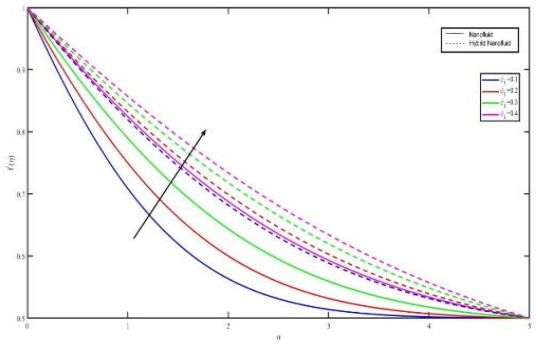

Figure 2. Effect of φ_1 on $f'(\eta)$ without magnetic effect.

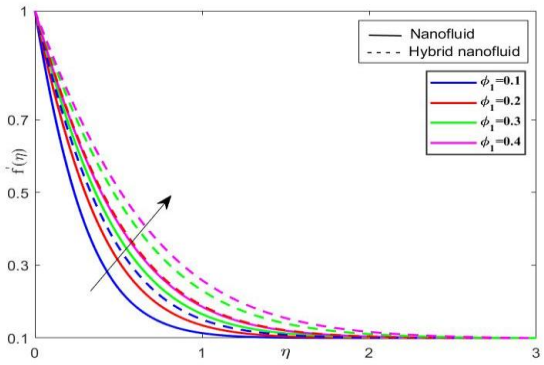

Figure 3. Effect of φ_1 on $f'(\eta)$.

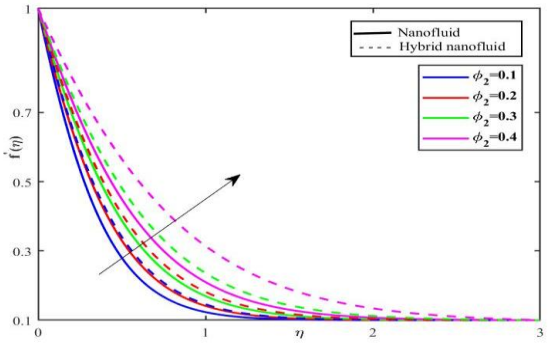

Figure 4. Effect of φ_2 on $f'(\eta)$.

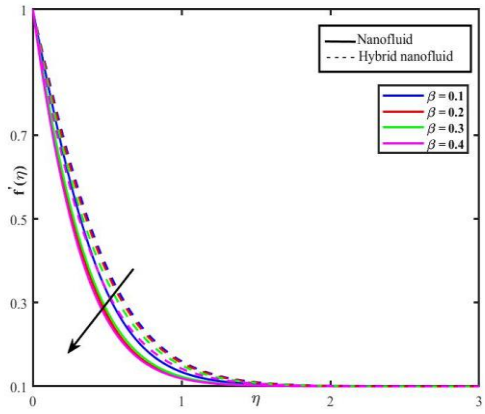

Figure 5. Effect of βon $f'(\eta)$.

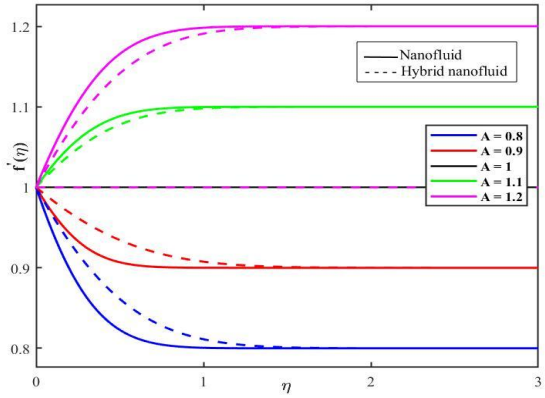

Figure 6. Effect of A on $f'(\eta)$.

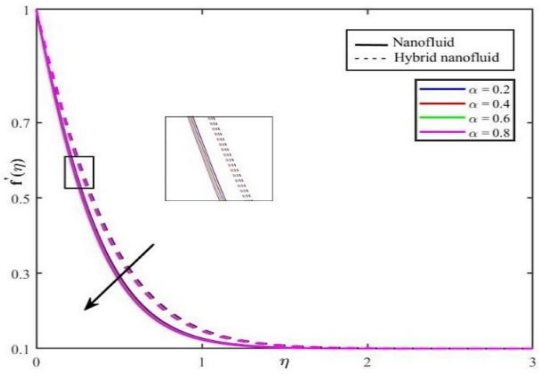

Figure 7. Effect of α on $f'(\eta)$.

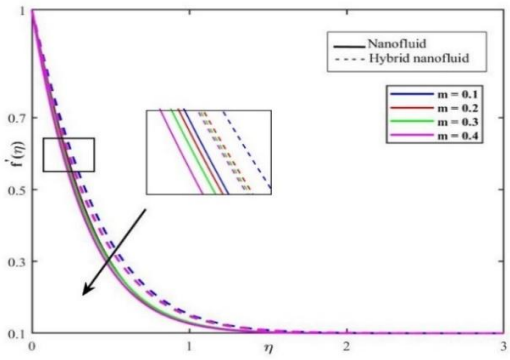

Figure 8. Effect of m on $f'(\eta)$.

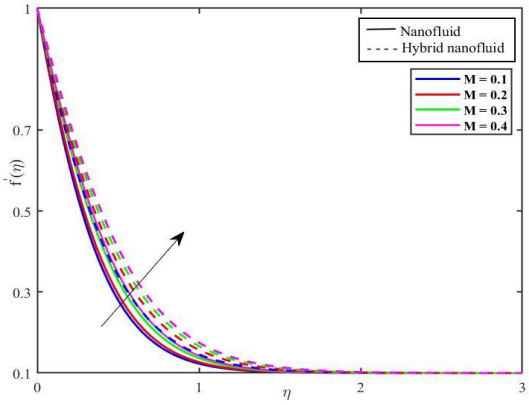

Figure 9. Effect of M on $f'(\eta)$.

Influence of significant parameters $(\varphi_1, \varphi_2, \beta, A, \alpha, m, M, Rd)$about temperature profile on $\theta(\eta)$.
Figure 10 and 11 depicts the variations corresponding to$\varphi_1 \in [0.1,0.4]$ and $\varphi_2 \in [0.1,0.4]$ on $\theta(\eta)$. Hybrid nanofluid, owing to its fractional particle size, exhibits significantly greater effects in comparison to regular nanofluid.Figure12 emphasizes the significance of temperature adjustments in response to variations in the radiation parameterRd $\in [0.1,0.4]$. It is evident that hybrid nanofluids yield more pronounced effects compared to pure nanofluid.Figure 13 demonstrates the variations in the influence of melting parameter $\beta \in [0.1,0.4]$ effects on $\theta(\eta)$, hybrid nanofluid exhibiting more pronounced effects compared to the nanofluid, primarily due to its elevated melting point.Figure 14 portrays the implications of $M \in [0.1,0.4]$ on the temperature profile, with the magnetic parameter of hybrid nanofluid which causes moreeffects compared to the nanofluid.Figure 15 illustrates how varying the Eckert number within the range of $Ec \in [0.1,0.4]$ affects the temperature profile and shows that hybrid nanofluids exhibit greater variations compared to convenctional nanofluids with changing Eckert numbers.

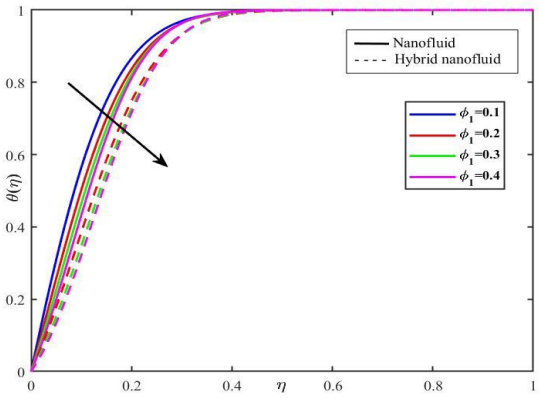

Figure 10. Effect of φ_1 on $\theta(\eta)$.

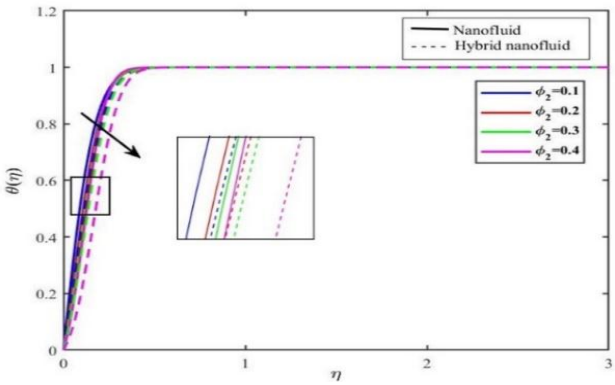

Figure 11. Effect of φ_2 on $\theta(\eta)$.

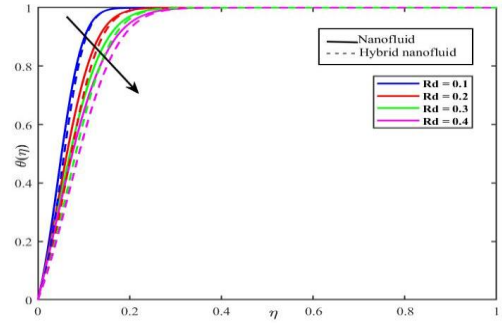

Figure 12. Effect of Rd on θ(η)

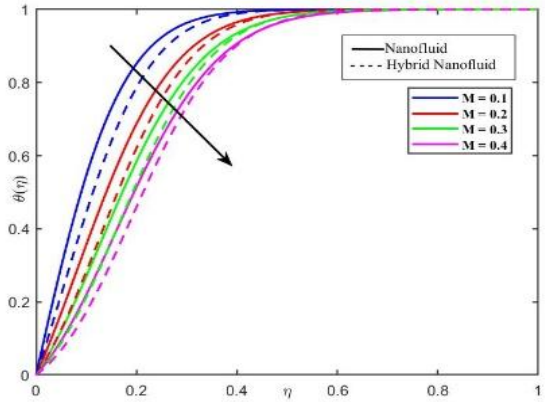

Figure 13. Effect of M on θ(η).

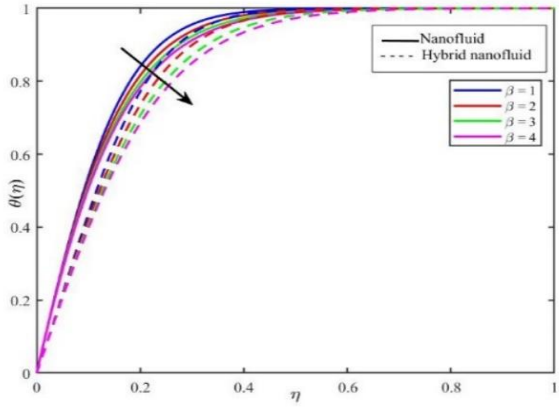

Figure 14. Effect of β on θ(η).

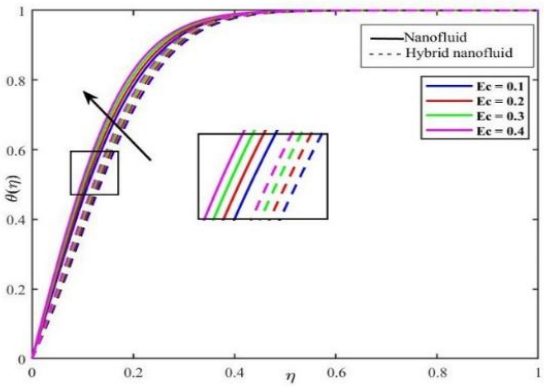

Figure 15. Effect of Ec on θ(η).

Influence of prominent parameters on wall shear stress and Nusselt number$S(C_f, Nu_x)$

To analyze the technological and industrial processes, it is essential to reduce the skin friction coefficient and improve the efficiency of Nusselt number.Consequently, in Figure. 16, 17, and 18&Figure. 19, 20 and 21 respectively, C_f and Nu_x are plotted for the influence of φ_1, φ_2&A, M&φ_2, β respectively. A can be set to higher levels to decrease the skin friction coefficientC_f. In the same way, higher values of φ_1, φ_2,A, M& β respectively, can regulate the nusselt number Nu_x.

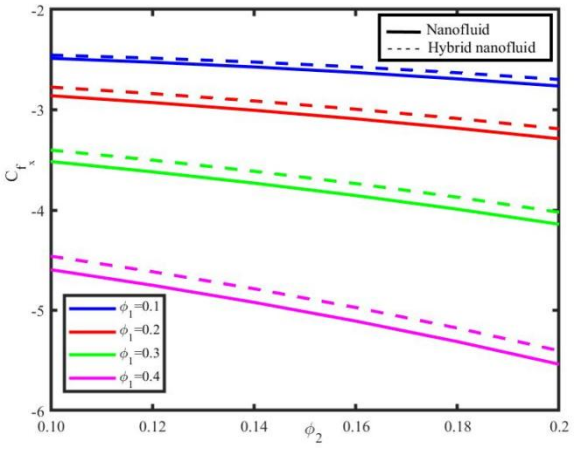

Figure 16. Effect of φ_1 and φ_2 on C_f.

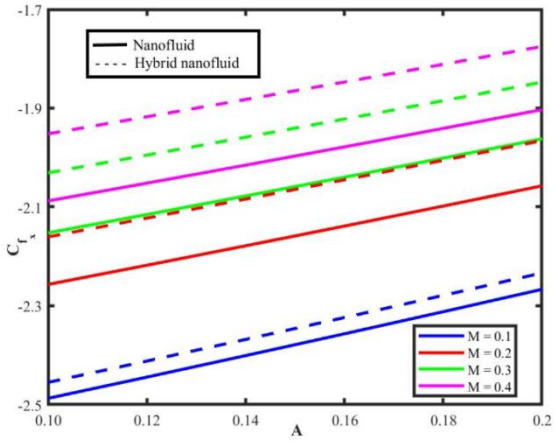

Figure 17. Effect of A and M on C_f.

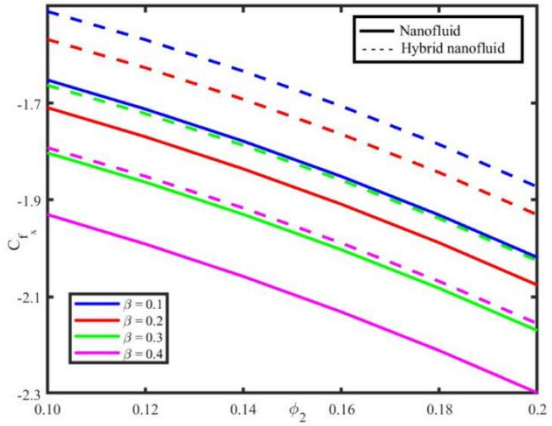

Figure 18. Effect of φ_2 and β on C_f.

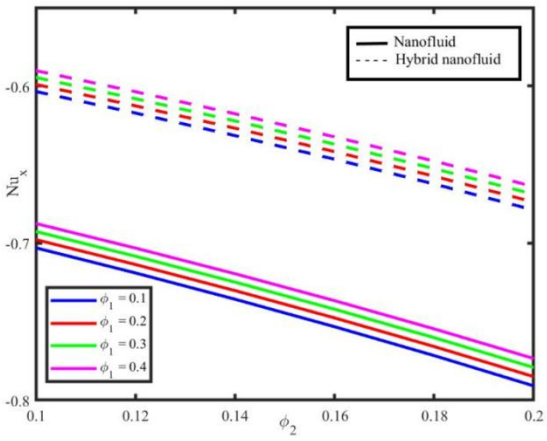

Figure 19. Effect of φ_2 and φ_1 on Nu_x.

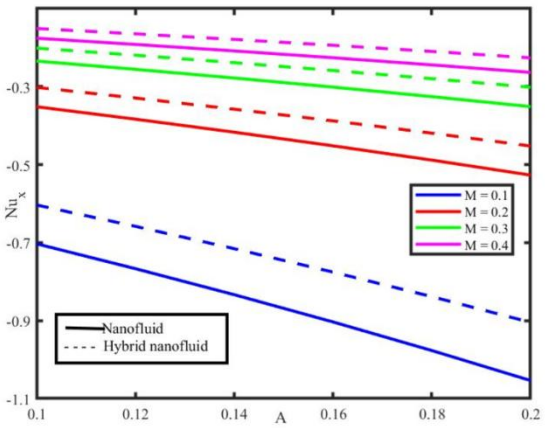

Figure 20. Effect of A and M on Nu_x.

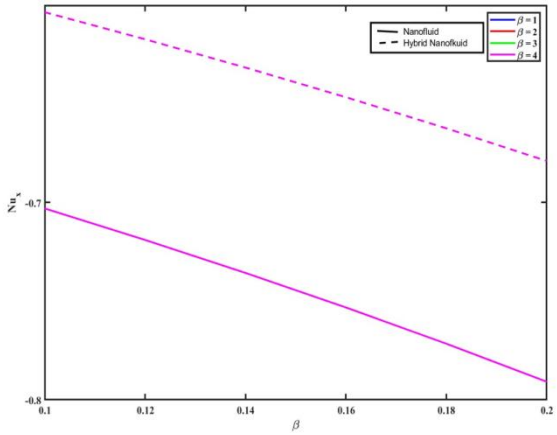

Figure 21. Effect of φ_2 and βon Nu_x.

CONCLUSION

The hybrid nanofluid flow of magnetohydrodynamics across a stretched sheet with different thicknesses is investigated in this work. A detailed explanation of the rate of heat transfer using MHD, melting heat and viscous dissipation is provided. A hybrid nanofluid can be developed by incorporating SWCNTs as 1st nanoparticle and Silver(Ag) as 2nd nanoparticle into the base fluid gasoline. To produce solutions using BVP4C techniques, the governing PDEs of flow are converted into the system of first order ODEs.The important findings of the present investigations are as follows.

- Velocity $f'(\eta)$ enhances with higher values of$\varphi_1, \varphi_2, \beta$, A while it decays for$\alpha$, m , M.
- Temperature $\theta(\eta)$ reduces for higher $\varphi_1, \varphi_2, \beta$, M and Rdand it becomes more intense with Ec.
- The skin friction coefficient decreases with higher values of A.

- By increasing the values of $\varphi_1, \varphi_2, \beta, A$ the cooling process (Nusselt number) may be effectively managed.

Visual walkthrough Graphical Abstract

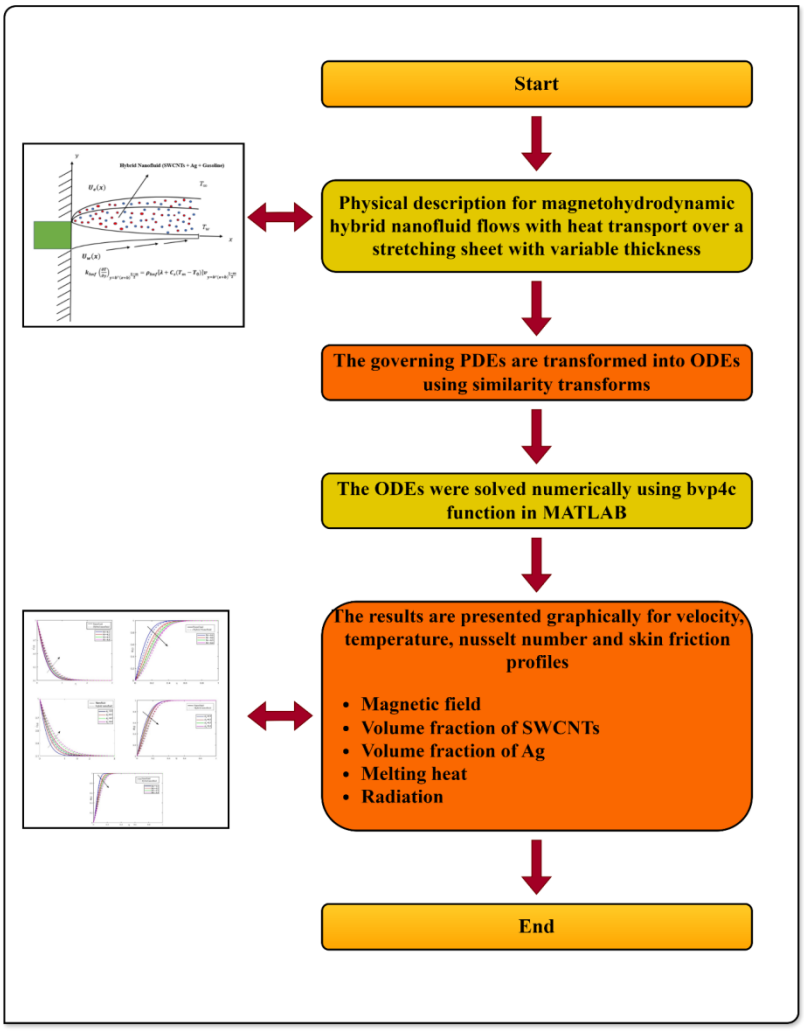

Figure 22. The flow chart shows a step-by-step workflow.

Nomenclature of physical expressions

u, v	velocity components
μ_f	dynamic viscosity (gasoline oil)
k_f	thermal conductivity (gasoline oil)
ρ_f	density (gasoline oil)
υ_f	kinematic viscosity (gasoline oil)
α_f	thermal diffusivity (gasoline oil)
m	behavior index parameter about flow
x, y	cartesian coordinates
A	velocity ratio parameter
f	non-dimensional velocity
θ	non dimensional temperature
T_w	wall temperature
T_m	surface temperature
T_∞	ambient temperature
q_w	wall heat flux
φ_1	volume fraction (SWCNTs)
φ_2	volume fraction (Ag)

C_s heat capacity (solid surface)
$(C_p)_f$ specific heat (gasoline oil)
Pr Prandtl Number
β melting parameter
α wall thickness parameter
U_0, U_∞ arbitrary constant
U_e free stream velocity
τ_w wall shear stress
U_w stretching velocity
λ latent heat
CNTs carbon nanotubes
M magneto hydrodynamic
Ec Eckert number
Rd Radiation
n nanoparticle shape
k_{s1} thermal conductivity (SWCNTs)
k_{s2} thermal conductivity (Ag)

For nanofluid

k_{nf} thermal conductivity
α_{nf} thermal diffusivity
$(C_p)_{nf}$ specific heat
μ_{nf} dynamic viscosity
υ_{nf} kinematic viscosity
ρ_{nf} density

For hybrid nanofluid

k_{hnf} thermal conductivity
α_{hnf} thermal diffusivity
$(C_p)_{hnf}$ specific heat
μ_{hnf} dynamic viscosity
υ_{hnf} kinematic viscosity
ρ_{hnf} density

REFERENCES

[1] Choi SUS, and Jeffrey Eastman A. Enhancing thermal conductivity of fluids with nanoparticles. Argonne National Lab. (ANL), Argonne, IL (United States), (1995),No. ANL/MSD/CP-84938; CONF-951135-29.
[2] VajraveluK.Viscous flow over a nonlinearly stretching sheet, Appl. Math. Comput., (2001), vol. 124, pp. 281–288.
[3] Fang T, Zhang J,Zhong Y.Boundary layer flow over a stretching sheet with variable thickness. Appl Math Comput (2012), 218,7241–52.
[4] Anjali Devi SPand Prakash M. Thermal radiation effectson hydromagnetic flow over a slandering stretching sheet. Journal of the Brazilian society of mechanical sciences and engineering (2016),38,423-431.
[5] Volder MFLD, Tawfick SH, Baughman RH, Hart AJ, Carbon nanotubes: present and future commercial applications, Science (2013), 339, 535–539.
[6] Muhammad K, Hayat T, Alsaedi A and Asghar S, Stagnation point flow of basefluid(gasoline oil), nanomaterial (CNTs) and hybrid nanomaterial (CNTs+ CuO): a comparative study, Mater. Res. Express. (2019),6,105003(1-24).
[7] Turkyilmazoglu. M, Natural convective flow of nanofluids past a radiative and impulsive vertical plate, J. Aerosp. Eng. (2016), 29, 1–8.
[8] Mami Nassima, Mohamed Najib Bouaziz. Effect of MHD on Nanofluid Flow, Heat, Mass Transfer over a Stretching Surface Embedded in a Porous Medium. PeriodicaPolytechnica Mechanical Engineering (2018),62 (2),91-100.
[9] Seikh A, Akinshilo A,Taheri M H, Gorji M R, Alharthi N H, Khan I, Khan A R, Influence of the nanoparticles and uniform magnetic field on the slip blood flow in arterial vessels, Phys. Scr. (2019),94(12), 125218(1-18).

[10] Goud B S, Srilatha P, Bindu P, and Krishna Y H, Radiation effect on mhd boundary layer flow due to an exponentially stretching sheet, Advances in Mathematics: Scientific Journal, (2020), 9(12), 10755–10761.
[11] Poply Vikas. Heat Transfer in a MHD Nanofluid Over a Stretching Sheet. Heat Transfer - Design, Experimentation and Applications. (2021),1,1-13.
[12] Prasad K V, Vajravelu K,Vaidya H&Van Gorder R A. MHD flow and heat transfer in a nanofluid over a slender elastic sheet with variable thickness. Results in physics, (2017), 7, 1462-1474.
[13] Suresh S, Venkitaraj K P,Selvakumar P, and Chandrasekar M, Synthesis of Al2O3–cu/water hybrid nanofluids using two step method and its thermo physical properties, Colloids and Surf. A (2011), 388, 41–48.
[14] Ahmad S, Nadeem S, &Khan M N.Enhanced transport properties and its theoretical analysis in two-phase hybrid nanofluid. Appl Nanosci (2022), 12, 309–316.
[15] Anjali Devi S P, Suriya Uma Devi S. Numerical Investigation of Hydromagnetic Hybrid Cu – Al2O3/Water Nanofluid Flow over a Permeable Stretching Sheet with Suction. International Journal of Nonlinear Sciences and Numerical Simulation, (2016), 17(5), 249-257.
[16] Hayat T,Nadeem S, Heat transfer enhancement with Ag-CuO/water hybrid nanofluid, Results Phy. (2017),7, 2317–2324.
[17] Waini I,Ishak A, and Pop I, Hybrid nanofluid flow induced by an exponentially shrinking sheet, Chinese Journal of Physics, (2020), 68, 468–482.
[18] Roberts L, On the melting of a semi-infinite body of ice placed in a hot stream of air, J. Fluid Mech. (1958), 4, 505–528.
[19] Hayat T, Muhammad K, Farooq M, Alsaedi A, Melting heat transfer in stagnation point flow of carbon nanotubes towards variable thickness surface, AIP Adv. (2016),6, 015214(1-14).
[20] Mabood F, Mastroberardino, Antonio. Melting heat transfer on MHD convective flow of a nanofluid over a stretching sheet with viscous dissipation and second order slip. Journal of the Taiwan Institute of Chemical Engineers, (2015),57,62-68.
[21] Zainal, Nurul Amira, Roslinda Nazar, KohilavaniNaganthran, and Ioan Pop. MHD flow and heat transfer of hybrid nanofluid over a permeable moving surface in the presence of thermal radiation.International Journal of Numerical Methods for Heat & Fluid Flow (2021), 31(3),858-879.
[22] Shafiq, Anum, Ilyas Khan, Ghulam Rasool, El-Sayed M. Sherif, and Asiful H. Sheikh. Influence of Single- and Multi-Wall Carbon Nanotubes on Magnetohydrodynamic Stagnation Point Nanofluid Flow over Variable Thicker Surface with Concave and Convex Effects. Mathematics (2020),8(1),104.
[23] A'isyahJ, Iskandar W, Anuar J, Roslinda N, Ioan Pop. MHD flow and heat transfer of a hybrid nanofluid past a nonlinear surface stretching/shrinking with effects of thermal radiation and suction, Chinese Journal of Physics. (2022), 79, 13-27.
[24] Rammoorthi, Rajakumari, and Dhivya Mohanavel. Influence of Radiative Magnetic Field on a Convective Flow of a Chemically Reactive Hybrid Nanofluid over a Vertical Plate. Journal of Advanced Research in Fluid Mechanics and Thermal Sciences (2023), 105(1), 90-106.
[25] Muhammad K, Hayat T, and Alsaedi A. Numerical study for melting heat in dissipative flow of hybrid nanofluid over a variable thicken surface. International Communications in Heat and Mass Transfer(2021),121,104805(1-10).
[26] Abdul Basit, Muhammad Zahid, Grzegorz Liśkiewicz. Analysis of MHD hybrid nanofluid through an exponential stretching sheet with dissipation and radiation effects. TechRxiv.(2023),6,1-25.
[27] Jamrus, Farah Nadzirah, Iskandar Waini, Umair Khan, and Anuar Ishak. Effects of magnetohydrodynamics and velocity slip on mixed convective flow of thermally stratified ternary hybrid nanofluid over a stretching/shrinking sheet. Case Studies in Thermal Engineering (2024),55,104161(1-19).